Decoupled Dynamics and Quasi-Logarithmic Relaxation in the Polymer−Plasticizer System Poly(methyl methacrylate)/Tri-*m*-cresyl Phosphate Studied with 2D NMR

Dieter Bingemann,† Nadine Wirth, Jürgen Gmeiner, and Ernst A. Rössler*

Experimentalphysik II, Universität Bayreuth, 95447 Bayreuth, Germany

Received March 2, 2007; Revised Manuscript Received May 2, 2007

ABSTRACT: Studying the dynamics of the polymer−plasticizer system poly(methyl methacrylate) (PMMA)/tri-*m*-cresyl phosphate (TCP), we find pronounced dynamic heterogeneities for the additive TCP with one- and two-dimensional ^{31}P NMR spectroscopy, whereas the dispersion of the dynamics of the polymer PMMA, studied simultaneously with ^{2}H NMR, remains essentially unchanged upon addition of the plasticizer TCP, despite a large decrease in the correlation time. TCP molecules reorient isotropically even in a rigid polymer matrix at temperatures well below the glass transition of the plasticized PMMA. Taking advantage of the very large time window accessible with the stimulated echo technique for the ^{31}P nucleus, we show that the orientational correlation functions of TCP change from Kohlrausch decays for pure TCP to quasi-logarithmic decays in the mixture, which resemble those from recent simulations with a bead-and-spring model [Moreno, A. J.; Colmenero, J. *J. Chem. Phys.* **2006,** *124,* 184906]. Two-dimensional spectra for TCP show that the dynamic heterogeneities of the plasticizer are transient in nature.

1. Introduction

Binary glassy systems, such as polymer blends, copolymers, or plasticized polymers, open the door to an almost unlimited fine-tuning of material properties. For example, a polyurethane−poly(ethylene glycol) block copolymer is behind the stretchy sports fabric well-known under the trade name Spandex, car tires are made of a butadiene−styrene copolymer, and phthalate plasticizers soften poly(vinyl chloride) for upholstery.[1] Block copolymers even offer a feasible path to holographic data storage systems.[2] Because of their widespread use, the dynamics of these binary glasses is of great technological importance for issues ranging from their processing behavior to material fatigue and even the diffusion of the plasticizer di(2-ethylhexyl) phthalate (DEHP) out of children's toys and medical supplies.

The dynamics of polymer blends, block copolymers, and plasticized polymers are significantly more complex than those of homopolymers. For example, depending on the difference in the glass transition temperature, T_g, of the two components,[3] very broad or bimodal spectra are observed in dielectric spectroscopy,[4−8] glass transitions are either broadened or show two steps in calorimetric measurements,[9−13] and NMR relaxation time scales broaden significantly[8,14−16] (for reviews see refs 17 and 18). As a consequence, pronounced dynamic heterogeneities are typical for these systems and were observed even in binary low-molecular-weight glasses.[8,16−18] Often, the frequency−temperature superposition principle fails in these systems. Concentration fluctuations[19−21] and self-concentration effects[22,23] due to chain connectivity in combination with decoupled dynamics of the two components[23,24] were proposed to explain this broadening on a molecular scale.

Pure glass-forming liquids typically show two-step correlation functions with clearly distinguishable fast and slow relaxation contributions. However, applying a bead-and-spring model, recent numerical simulations of the correlation function for the fast component in a polymer blend[25,26] found a very unusual, highly stretched, relaxation with no discernible relaxation plateau separating fast and slow dynamics. Decreasing temperature led to a convex-to-concave transition of the correlation function with a quasi-logarithmic decay for intermediate temperatures. The authors interpreted this behavior as a signature of the confinement of the fast component in a slow matrix in addition to its kinetic arrest by neighboring molecules of the same kind,[25,26] suggesting that, in addition to the dynamic heterogeneity of one-component systems, these binary glassy systems also exhibit structural heterogeneities. A lattice model incorporating these structural heterogeneities has been used to explain a bimodal distribution of the diluent dynamics in an experimental study on plasticized polycarbonate.[27]

Quasi-logarithmic dynamics were reported for a number of theoretical and experimental studies of binary systems. Logarithmic relaxation functions were found in simulations of kinetically constrained glass model systems,[25,26,28] were observed in neutron scattering experiments in polymer blends,[29] and are also predicted with higher order transitions within mode coupling theory for short-range attractive colloids.[30] Very slow, logarithmic, decays were even observed in the loss of macroscopic orientational order in the holographic data storage systems mentioned above.[2]

In this paper we describe detailed nuclear magnetic resonance (NMR) experiments on a binary glass-former, poly(α-deuterated methyl methacrylate) (PMMA-d_3), plasticized with tri-*m*-cresyl phosphate (TCP), two components with very different glass transition temperatures. With ^{2}H and ^{31}P NMR we can follow the dynamics of both components individually in the same sample and compare the results to the behavior of the pure components. (Details of the experiments on pure TCP were published previously.[31]) The relaxation of TCP changes from Kohlrausch decays for pure TCP to quasi-logarithmic decays in the mixture, which resemble those from simulations.[25,26] We are able to monitor the extremely stretched relaxation of TCP in the mixture because of the broad time window of the stimulated echo technique for the ^{31}P nucleus, covering 7−8

* Corresponding author. E-mail: ernst.roessler@uni-bayreuth.de.
† On leave from Department of Chemistry, Williams College, 47 Lab Campus Drive, Williamstown, MA 01267.

10.1021/ma070519g CCC: $37.00
Published on Web 06/28/2007

decades in time, which is significantly larger than the time window accessible with ^{2}H NMR in most cases. With one- and two-dimensional NMR spectroscopy, we show that the dynamic heterogeneities of the plasticizer TCP are transient in nature and occur even in an essentially rigid matrix of PMMA.

2. NMR Background

2.1. 1D Spectra. The NMR frequency depends on the angle θ_λ between the principal interaction tensor axis and the magnetic field direction:

$$\omega(\theta_\lambda) = \delta_\lambda/2(3\cos^2\theta_\lambda - 1) \quad (1)$$

where $\omega(\theta_\lambda)$ is the shift of the resonance frequency with respect to the Larmor frequency, ω_L. The parameter δ_λ specifies the anisotropy of the interaction tensor, which is given by the chemical shift anisotropy (CSA) in the case of ^{31}P. For ^{2}H NMR in PMMA-d_3, rapid rotation of the CD_3 groups reduces the rigid-lattice spectral width as determined by the quadrupole interaction tensor by a factor of about 3. Both interaction tensors are axially symmetric. Since ^{2}H is a spin $I = 1$ nucleus, two NMR frequencies are observed at $\omega = \omega_L \pm \omega(\theta_\lambda)$, leading to a symmetric spectrum, whereas the CSA powder spectrum is asymmetric. For ^{2}H NMR the principal interaction tensor axis corresponds to the C−CD_3 bond in PMMA-d_3, while for ^{31}P NMR it is given by the symmetry axis of the PO_4 entity in the TCP molecule. In samples with an isotropic orientational distribution of immobile molecules (e.g., glasses), eq 1 leads to a characteristic powder spectra; in the case of ^{2}H NMR one finds the famous Pake spectrum.[32] These broad solid-state spectra require measurements with an echo-pulse sequence, in particular a Hahn echo for ^{31}P ($I = 1/2$) and a solid-echo for ^{2}H ($I = 1$).

Upon heating above the glass transition temperature, accelerated isotropic reorientation shortens the correlation time, τ, leading finally to a continuous collapse of the powder spectrum line shape into a central narrow line for many pure glass-formers. In contrast, in binary glasses the distribution of correlation times, $G(\ln\tau)$, is broader, in particular for the more mobile component, and one observes a superposition of a liquidlike Lorentzian spectrum and a solid-state powder spectrum with temperature-dependent weighting factors.[8,14−18] This superposition is often referred to as a "two-phase" spectrum[17] despite the fact that the mixture is homogeneous and not phase-separated. In this case the contributions to the spectrum from molecules with intermediate relaxation times, $\tau \cong 1/\delta_\lambda$, can be neglected, and only the spectra for the fast ($S_{Lor}(\omega)$, $\tau \ll 1/\delta_\lambda$) and slow ($S_{powder}(\omega)$, $\tau \gg 1/\delta_\lambda$) motion limit need to be taken into account. The total (solid-echo or Hahn-echo) spectrum can simply be written

$$S(\omega;T) = S_{Lor}(\omega)W(T) + S_{powder}(\omega)(1 - W(T)) \quad (2)$$

where $W(T)$ is a temperature-dependent weighting factor changing from zero to one as the distribution $G(\ln\tau)$ shifts toward shorter correlation times upon heating.

2.2. Stimulated Echo Experiments. Quantitative information about the reorientation dynamics can be gained from stimulated echo experiments. A three-pulse echo sequence is applied (cf. Experimental Section), and the echo amplitude is monitored as a function of the mixing time, t_m, for a constant delay between the first two pulses, t_p (evolution time). The echo amplitude reads

$$I(t_m,t_p) \propto \langle \sin(\omega(0)t_p)\sin(\omega(t_m)t_p)\rangle \exp(-(t_m/T_\lambda)^{\beta_\lambda}) \quad (3)$$

The factor in angle brackets represents the orientational correlation function $F_{t_p}^{sin}(t_m)$, and the exponential term is a damping factor caused by NMR relaxation effects. For the ^{31}P nucleus, T_λ is given by the spin−lattice relaxation time, T_1 (with $\beta_\lambda = 1$), and for the ^{2}H nucleus by the quadrupolar relaxation time constant, T_{1Q}, with $\beta_\lambda < 1$. This damping represents an upper limit for the accessible time window in stimulated echo experiments. The slow and exponential spin−lattice relaxation of the ^{31}P nucleus allows to follow the correlation loss of TCP over 8 orders of magnitude in time, from 1 μs to 100 s, while the much shorter quadrupole relaxation time of the ^{2}H nucleus limits the measurements in PMMA to a maximum mixing time, t_m, of about 10 ms.

The orientational correlation function $F_{t_p}^{sin}(t_m)$can be normalized according to[33]

$$F_{t_p}^{sin}(t_m) = [1 - F_\infty(t_p)]\phi_{t_p}(t_m) + F_\infty(t_p) \quad (4)$$

where $\phi_{t_p}(t_m)$ denotes the normalized relaxation function, describing the loss of correlation caused by the motional process, while $F_\infty(t_p)$ stands for the residual correlation which does not relax. The value of the latter quantity depends on the geometry of the reorientational mechanism and is well documented for the isotropic motion encountered in this work.[33]

In the case of isotropic reorientation, for short delay times, t_p, the residual correlation $F_\infty(t_p)$ approaches 0, and the normalized correlation function, $\phi_{t_p}(t_m)$, approximates the frequency−frequency correlation function, $\langle\omega(0)\omega(t_m)\rangle$

$$\lim_{t_p\to 0}\phi_{t_p}(t_m) \propto \langle\omega(0)\omega(t_m)\rangle \propto F_2(t_m) \quad (5)$$

which is proportional to the orientation correlation function of the second Legendre polynomial, $F_2(t_m)$, via eq 1. For the pure components as well as for PMMA in the binary mixture with TCP we approximate the correlation function $F_2(t_m)$ with a stretched exponential function (Kohlrausch decay):

$$F_2(t_m) = \exp(-(t_m/\tau_K)^{\beta_K}) \quad (6)$$

The mean correlation time, τ, depends on the time constant, τ_K, and the stretching parameter, β_K, according to

$$\tau = \tau_K\Gamma(1/\beta_K)/\beta_K \quad (7)$$

where $\Gamma(x)$ signifies the gamma function.

2.3. 2D Spectra. A two-dimensional (2D) NMR spectrum, $S(\omega_1,\omega_2;t_m)$, measures the conditional probability, $P(\omega_2,t_m|\omega_1,0)$, to find a frequency ω_2 at time t_m if it was ω_1 at time $t = 0$.[34] Thus, 2D spectra provide a direct visualization of the evolution of the reorientation process. As in the stimulated echo experiments, three-pulse sequences with a mixing time, t_m, are applied[34] to determine the 2D ^{31}P spectra (cf. Experimental Section).

For a broad distribution of correlation times, $G(\ln\tau)$, a 2D spectrum can in the slow motion limit be described as a weighted superposition of a diagonal spectrum, $S_{dia}(\omega_1,\omega_2)$, representing immobile molecules, and a spectrum caused by complete isotropic reorientation, $S_{reo}(\omega_1,\omega_2)$ (Figure 1). For orientational relaxation through random orientational jumps the "two-phase" decomposition into the subspectra $S_{dia}(\omega_1,\omega_2)$ and $S_{reo}(\omega_1,\omega_2)$ holds independent of whether the distribution of relaxation times, $G(\ln\tau)$, is broad or not.[16] With $p_{dia}(t_m)$ and $p_{reo}(t_m)$ denoting

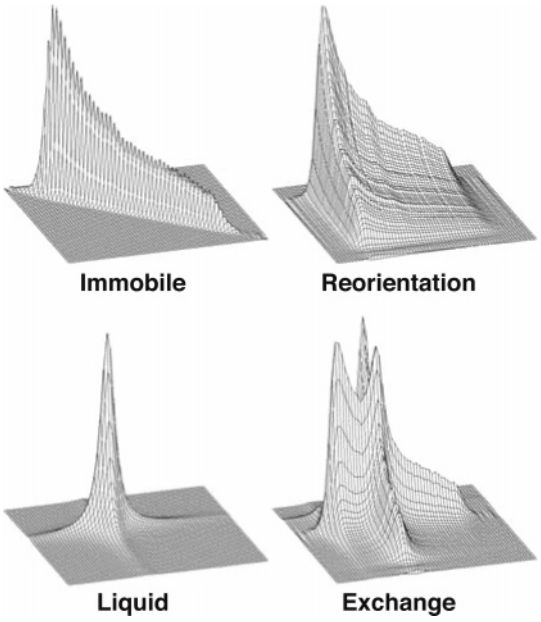

Figure 1. Calculated subspectra used to reproduce the 2D ^{31}P NMR spectra measured for TCP mixed with PMMA-d_3: $S_{dia}(\omega_1,\omega_2)$ 2D spectrum for immobile molecules ($\tau \gg t_m$, top left); $S_{reo}(\omega_1,\omega_2)$: for slowly reorienting molecules ($t_m \gg \tau \gg 1/\delta_{CSA}$, top right); $S_{Lor}(\omega_1,\omega_2)$: fast reorienting molecules ($\tau \ll 1/\delta_{CSA}$, bottom left); and $S_{ex}(\omega_1,\omega_2)$: for exchange between fast and slowly reorienting molecules. The frequency range depicted extends over 54 kHz along both axes.

the appropriate time-dependent weighting factors, the 2D spectrum can thus be written as

$$S(\omega_1,\omega_2;t_m) = p_{dia}(t_m)\, S_{dia}(\omega_1,\omega_2) + p_{reo}(t_m)\, S_{reo}(\omega_1,\omega_2) \quad (8)$$

with $p_{dia}(t_m) + p_{reo}(t_m) = 1$.[8,14] The reorientation spectrum, $S_{reo}(\omega_1,\omega_2)$, can be calculated from[14]

$$S_{reo}(\omega_1,\omega_2) = P_{powder}(\omega_1)\, P_{powder}(\omega_2) \quad (9)$$

where $P_{powder}(\omega)$ corresponds to the a priori probability for molecules to absorb the NMR frequency ω, which is given by the CSA powder spectrum. The diagonal spectrum, $S_{dia}(\omega_1,\omega_2)$, is given by the same a priori probability, $P_{powder}(\omega)$, along the diagonal of the spectrum:[8,14]

$$S_{dia}(\omega_1,\omega_2) = P_{powder}(\omega_1)\, \delta(\omega_1 - \omega_2) \quad (10)$$

where $\delta(x)$ stands for the delta function. At higher temperatures and for broad distributions of correlation times, the 1D spectra show a narrow line associated with fast molecules in addition to the powder spectrum reflecting slow molecules (eq 2). In this case two additional spectral contributions appear in the 2D spectra: a central Lorentzian peak, $S_{Lor}(\omega_1,\omega_2)$, which is an averaged 2D liquidlike pattern in analogy to the central line in the 1D spectrum, as well as a cross pattern, $S_{ex}(\omega_1,\omega_2)$, which stems from molecules that exchange their correlation time during the mixing time: fast molecules, relative to $1/\delta_\lambda$, become slow and vice versa (Figure 1). Thus, we can write[8,14,17,18]

$$S_{ex}(\omega_1,\omega_2) = P_{powder}(\omega_1)\, P_{liq}(\omega_2) + P_{liq}(\omega_1)\, P_{powder}(\omega_2) \quad (11)$$

where $P_{liq}(\omega)$ denotes the spectrum of the liquid line, usually a Lorentzian line shape. Thus, in this temperature range and in the limit of a broad distribution of relaxation times, the 2D spectrum can be described with a superposition of four subspectra, namely, $S_{dia}(\omega_1,\omega_2)$, $S_{reo}(\omega_1,\omega_2)$, $S_{Lor}(\omega_1,\omega_2)$, and $S_{ex}(\omega_1,\omega_2)$:[8,14,17,18]

$$S(\omega_1,\omega_2;t_m) = p_{dia}(t_m)\, S_{dia}(\omega_1,\omega_2) + p_{reo}(t_m)\, S_{reo}(\omega_1,\omega_2) + p_{Lor}(t_m)\, S_{Lor}(\omega_1,\omega_2) + p_{ex}(t_m)\, S_{ex}(\omega_1,\omega_2) \quad (12)$$

with $p_{dia}(t_m) + p_{reo}(t_m) + p_{Lor}(t_m) + p_{ex}(t_m) = 1$.

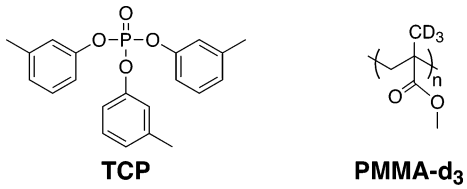

Figure 2. Molecular structures of tri-*m*-cresyl phosphate (TCP) and poly(α-deuteriomethyl methacrylate), PMMA-d_3.

3. Experimental Section

In this paper we investigate the dynamics of a sample of poly(α-deuterated methyl methacrylate) (PMMA-d_3) plasticized with tri-*m*-cresyl phosphate (TCP) (Figure 2) at a TCP concentration of 50.1% (w/w). The dynamics of the fast component, TCP, are monitored with ^{31}P NMR; PMMA-d_3, deuterated at the α-methyl group, is used to observe the dynamics of the polymer backbone separately with ^{2}H NMR in the same sample. Tri-*m*-cresyl phosphate (TCP) is used as received from Acros Organics (97%). PMMA-d_3 (Polymer Source, Montreal, Canada, $M_n = 23\,200$ g/mol, $M_w/M_n = 1.09$) is degassed under vacuum for 1 day at 100 °C. Equal amounts of TCP and PMMA-d_3 are weighed into an NMR tube, degassed, and homogenized under vacuum for 1 week and sealed off under vacuum. We do not observe any phase separation (cloudiness) in the mixture upon warming from liquid nitrogen temperatures.

Differential scanning calorimetry (DSC) was performed under nitrogen in a Netzsch DSC 200 instrument equipped with a liquid nitrogen cooling system. Typical sample amounts were about 10 mg. We measured the samples with a heating rate of 10 K/min.

The NMR measurements were performed in a Bruker DSX 400 spectrometer with a large core magnet and a field of 9.4 T corresponding to a Larmor frequency of 61.4 MHz for deuteron and 161.9 MHz for phosphorus. A Bruker VT 2000 temperature controller heated a flow of cold nitrogen gas to regulate the temperature of the sample to within 1 K. The accuracy of the temperature is about ±2 K.

We used a Hahn-echo two-pulse sequence with a delay time of $t_p = 30\ \mu$s to measure the ^{31}P 1D spectra. The anisotropy parameter is found to be $\delta_{CSA} = 2\pi$ 23.2 kHz for TCP. A three-pulse sequence, $(\pi/2)-t_p-(\pi/2)-t_m-(\pi/2)$, was applied to monitor the ^{31}P stimulated echo as a function of the mixing time, t_m. With the appropriate phases of the pulses[34] only the sine correlation function, $F_{t_p}^{sin}(t_m)$, is measured (cf. eq 3). For an evolution time of $t_p = 15\ \mu$s we find $F_\infty(t_p) = 0.03$. This final correlation value, $F_\infty(t_p)$, has to be taken into account to obtain the orientational correlation function, $\phi_{tp}(t_m)$ (eq 4). Assuming that the limit of short delay times, t_p, is reached (eq 5), we regard the normalized stimulated echo correlation function, $\phi_{tp}(t_m)$, as an estimate for the orientation correlation function, $F_2(t_m)$. The 2D spectra were recorded in TPPI mode,[34] symmetrized, and convoluted with an approximately 1 kHz broad Gaussian. All ^{31}P NMR spectra were measured with broadband ^{1}H decoupling to remove the heteronuclear dipolar coupling.

^{2}H NMR 1D spectra were acquired using a solid-echo pulse sequence with a delay time of $t_p = 15\ \mu$s, and $\delta_Q = 2\pi$ 40.9 kHz is found for PMMA-d_3. We measured the sine correlation function for ^{2}H using a three-pulse sequence with appropriate pulse lengths. For an evolution time of $t_p = 15\ \mu$s we find $F_\infty(t_p) = 0.11$, and

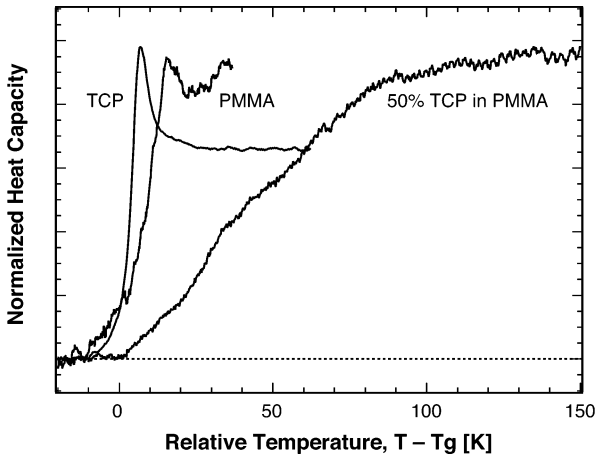

Figure 3. Differential scanning calorimetry (DSC) traces of PMMA, TCP, and a 50% (w/w) mixture of TCP in PMMA measured with a heating rate of 10 K/min. The traces are shifted by the experimentally determined glass transition temperatures, T_g, of 205 K (TCP), 381 K (PMMA), and 212 K (TCP/PMMA) as defined by the onset of the DSC step.

again we assume that the limit of eq 5 is reached, which may not be as good an assumption for ^{2}H NMR as it is for ^{31}P NMR.

Stimulated echo decays need to be corrected for the spin−lattice relaxation, T_1, in the case of ^{31}P NMR and for the quadrupolar relaxation, T_{1Q}, in the case of ^{2}H NMR (cf. eq 3). We determined the spin−lattice relaxation times, T_1, for ^{31}P NMR and ^{2}H NMR using the saturation-recovery technique with a two-pulse Hahn or solid-echo sequence, respectively, with fits to an exponential function in the case of ^{31}P NMR and to a stretched exponential in the case of ^{2}H NMR. The quadrupolar relaxation time, T_{1Q}, for ^{2}H NMR cannot be determined directly; instead, we define the decay of the stimulated echo at the lowest studied temperature as a pure T_{1Q} decay, fit it to a stretched exponential, and scale the resulting parameters T_{1Q} and β_Q according to the temperature dependence of the measured T_1 decay. We apply complete phase cycling[34,35] in all NMR experiments.

4. Results

4.1. Differential Scanning Calorimetry. The distinct behavior of polymer−plasticizer systems is immediately obvious in their thermal properties.[9−13] Comparing the differential scanning calorimetry (DSC) traces of the mixture of 50% (w/w) TCP in PMMA with those of the pure components, TCP and PMMA (Figure 3), we find a wide temperature range over which the heat capacity of the binary sample increases, i.e., a very broad "glass step". Here, T_g is defined as the onset temperature of the heat capacity step, and we determined $T_g \cong$ 205 K for pure TCP, $T_g \cong$ 381 K for pure PMMA, and $T_g \cong$ 212 K for the mixture. The end of the heat capacity increase for the mixture is reached at $T_G \cong$ 297 K. Thus, in the case of the mixture the freezing of the different degrees of freedom extends over 85 K, and a single glass temperature is not adequate to characterize the behavior of the heat capacity; rather, one needs to consider the entire temperature interval T_g to T_G. This wide temperature range already suggests an extreme broadening of the time scales of the dynamics in the mixture.

4.2. Temperature Dependence of the 1D Spectra. The complex dynamics of the binary mixture can be studied by observing the two components individually with ^{2}H and ^{31}P NMR spectroscopy. In 1D NMR spectra, the main signature of increased orientational motion at higher temperatures is the collapse of the powder spectrum into a single central line once the orientational correlation time of the molecule (or the polymer segment) drops below the inverse of the coupling constant: $\tau < 1/\delta_\lambda \approx 5 \times 10^{-6}$ s. This transition as a function of temperature can be seen in Figure 4 for the two components TCP (^{31}P NMR) and PMMA(^{2}H NMR), both in the mixture and individually as pure substances. The glass transition temperature, T_g, of PMMA is too high to record the complete collapse of the spectrum for pure PMMA, but the initial signature of the collapse can clearly be seen.

The figure already reveals three interesting facts about the mixture: First, the solid-state spectra for the two components in the binary mixture collapse to a Lorentzian line at quite different temperatures, indicating a pronounced decoupling of the dynamics of TCP and PMMA in the mixture. Tentatively, one can assign a separate and distinct glass transition temperature to each component in the mixture, about 60−70 K apart. Second, the collapse of the spectra for each component in the mixture is shifted with respect to the pure component, upward by 50 K in the case of TCP and downward by about 100 K in the case of PMMA. Third, at around 320 K we record a central line for the plasticizer TCP, indicating liquidlike behavior, while the matrix displays the powder spectrum of a rigid solid at the same temperature.

Furthermore, at the slightly lower temperature of around 280 K, we recorded spectra for TCP which can be described by a sum of the corresponding powder spectrum with a liquid Lorentzian line (eq 2) as indicated for one spectrum in Figure 4. This superposition ("two-phase spectrum") indicates a broad distribution of correlation times and is usually not observed in neat low molecular weight glass-formers as evident in the spectra for pure TCP in Figure 4. The appearance of two-phase spectra in particular for TCP in the mixture covering about 30 K is a clear indication of pronounced dynamic heterogeneities. Since this crossover to the liquid line occurs at temperatures for which the PMMA spectra are given by the powder spectrum of rigid molecules, these heterogeneities occur in a matrix of essentially rigid PMMA molecules.

Further insight into the dynamics of the PMMA matrix in the binary mixture can be gained from 1D spectra recorded with various delay times, t_p, between the two pulses in the solid-echo pulse sequence (Figure 5, right). Between 240 and 300 K no fast, large-scale angular motions are present; we observe only solidlike powder spectra. The loss of intensity at the center of the spectrum with increasing delay time, t_p, is the signature of small-angle motion still present in the polymer matrix, which plays an important role in the glass transition.[17,18,36,37] Comparing these spectra with those for pure PMMA (Figure 5, left), we find no qualitative difference, and we conclude that no additional motion is introduced by the embedded TCP. This apparent decoupling is quite surprising, as it is difficult to imagine a large molecule, such as TCP, reorienting isotropically in the PMMA matrix without affecting these aspects of the polymer dynamics.

4.3. 2D Spectra of TCP. The nature of the dynamic heterogeneities of TCP in the mixture with PMMA can be explored by measuring 2D ^{31}P NMR spectra at different mixing times, t_m. Since this mixing time is essentially only limited by the spin−lattice relaxation time, T_1, which is about 10−100 s for ^{31}P in our temperature range, we are able to access mixing times up to 5 s with good signal intensities. Accordingly, the dynamics can be probed on a time scale from microseconds to seconds, and dynamics slower than those observable with 1D experiments can be followed. Molecules that do not reorient during the mixing time, t_m, show an unchanged resonance frequency, $\omega_1 = \omega_2$, and their spectral contribution appears along the diagonal of the spectrum. In the other extreme, unrestricted

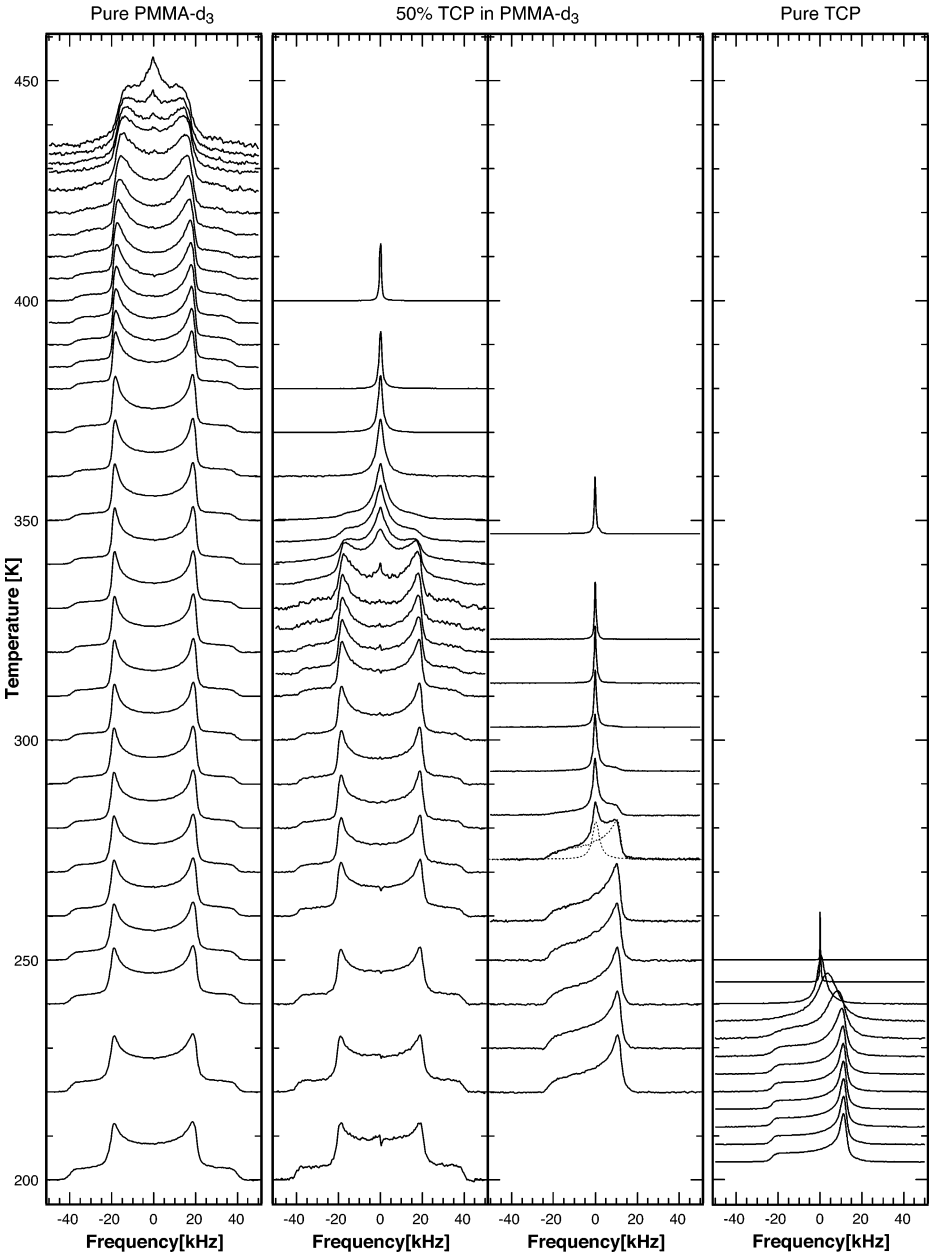

Figure 4. ^{2}H (left and center left) solid-echo and ^{31}P (right and center right) Hahn-echo NMR spectra for PMMA-d_3, (left), a 50% (w/w) mixture of tri-*m*-cresyl phosphate, TCP, with PMMA-d_3 (center), and pure TCP (right) from 200 to 435 K.

isotropic reorientation leads to the 2D equivalent of a powder spectrum where all cuts parallel to the frequency axes match the 1D powder spectrum shape (Figure 1).

A 2D spectrum of TCP with a mixing time of $t_m = 5$ s is shown in Figure 6 (left) for a temperature of 257 K. (For reference, this temperature is below the onset of the liquid line in the TCP 1D spectra displayed in Figure 4.) In addition to a small contribution along the diagonal, one observes strong off-diagonal intensity covering the entire accessible spectral range. The latter contribution to the spectrum is typical for an isotropic reorientation. The 2D spectrum also reveals a broad distribution of correlation times: after a waiting time of $t_m = 5$ s the majority of the molecules has reoriented isotropically, whereas a smaller fraction has not yet moved at all. Applying eqs 8−10, we can simulate the 2D spectrum as shown in Figure 6 (right). This simple model describes the experimental 2D spectrum well for $p_{dia} = 0.1$; i.e., about 10% of the TCP molecules in the mixture have not yet reoriented after 5 s at 257 K.

At 276 K, in the region of the "two-phase spectra" for TCP, the 2D spectrum is more complex, as shown in Figure 7 (left) for five different mixing times, t_m, ranging from 1 ms to 2 s. In addition to the diagonal spectrum indicating immobile molecules and the spectral contribution caused by isotropically reorienting molecules (Figure 6), we here also observe a liquid line as well as a crosslike pattern originating from exchange between "fast" molecules (liquid line) and "slow" molecules (powder spectrum), as shown in Figure 1. A qualitative inspection of the experimental spectra shows that the exchange and the reorientation component grow at about the same rate, while the contributions from the liquid line and the diagonal decrease accordingly. Furthermore, the exchange/reorientation dynamics extends over many orders of magnitude in time; i.e., the corresponding correlation function is highly stretched with some exchange already visible at the shortest waiting time of $t_m = 1$ ms, while some molecules are still stationary after the longest waiting time of $t_m = 2$ s.

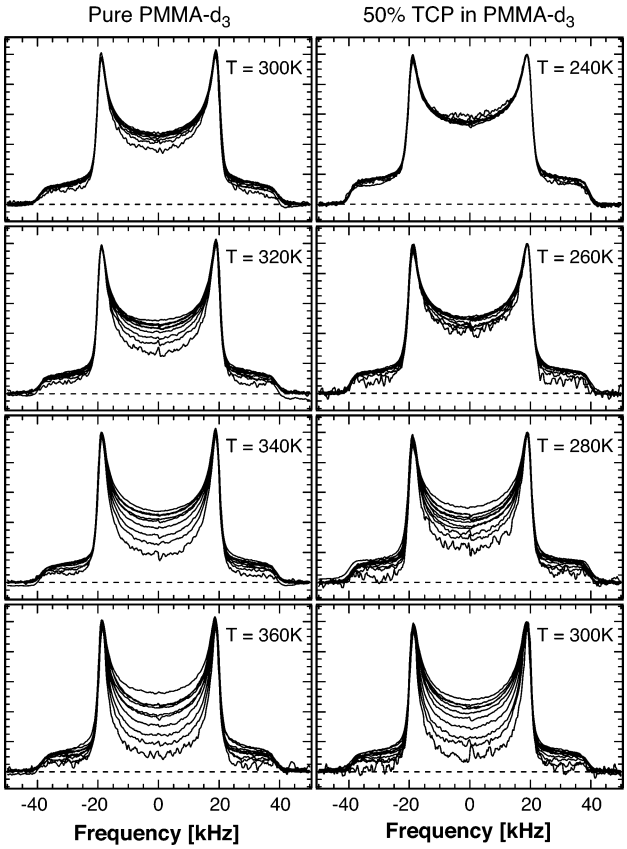

Figure 5. ^{2}H solid-echo NMR spectra for PMMA-d_3, (left) and a 50% (w/w) mixture of tri-*m*-cresyl phosphate, TCP, with PMMA-d_3 (right) from 300 to 360 K and from 240 to 300 K, respectively, for interpulse delays, t_p, from 10 to 300 μs.

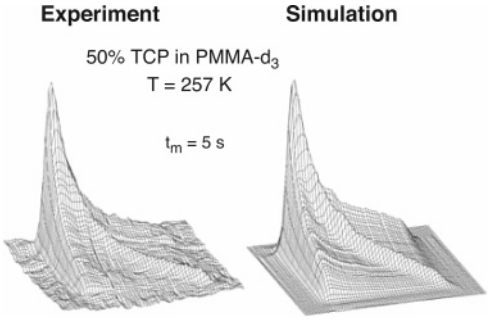

Figure 6. 2D ^{31}P NMR spectrum of a 50% (w/w) mixture of tri-*m*-cresyl phosphate, TCP, with PMMA-d_3 at 257 K for a mixing time of $t_m = 5$ s (left). A simulation based on the 1D ^{31}P Hahn-echo spectrum assuming complete reorientation for 90% of the TCP molecules is shown on the right (cf. eq 8). The frequency range depicted extends over 54 kHz along both axes.

In a quantitative analysis, we fit each experimental 2D spectrum as a weighted sum of the four individual components (Figure 1 and eqs 11 and 12), as shown on the right in Figure 7, confirming our qualitative assessment of the dynamics. The weighting factors p_{dia}, p_{reo}, and p_{ex} are shown as a function of the mixing time, t_m, in Figure 8. At $t_m = 0$, reorientation and exchange have not yet taken place; thus, $p_{reo} = 0$ and $p_{ex} = 0$. The weighting factor for the diagonal component, p_{dia}, at $t_m = 0$ is identical to the powder contribution to the 1D spectrum at the same temperature as given by eq 2: $p_{dia} = 1 - W(T) = 0.38$. Likewise, the weighting factor for the diagonal component, p_{dia}, at long times, $t_m = \infty$, vanishes, while p_{ex} is related to $W(T)$ according to $p_{ex} = 2W(T)(1 - W(T))$.[14] These limiting values, calculated from the corresponding 1D ^{31}P NMR spectrum, are indicated in Figure 8 with arrows. As

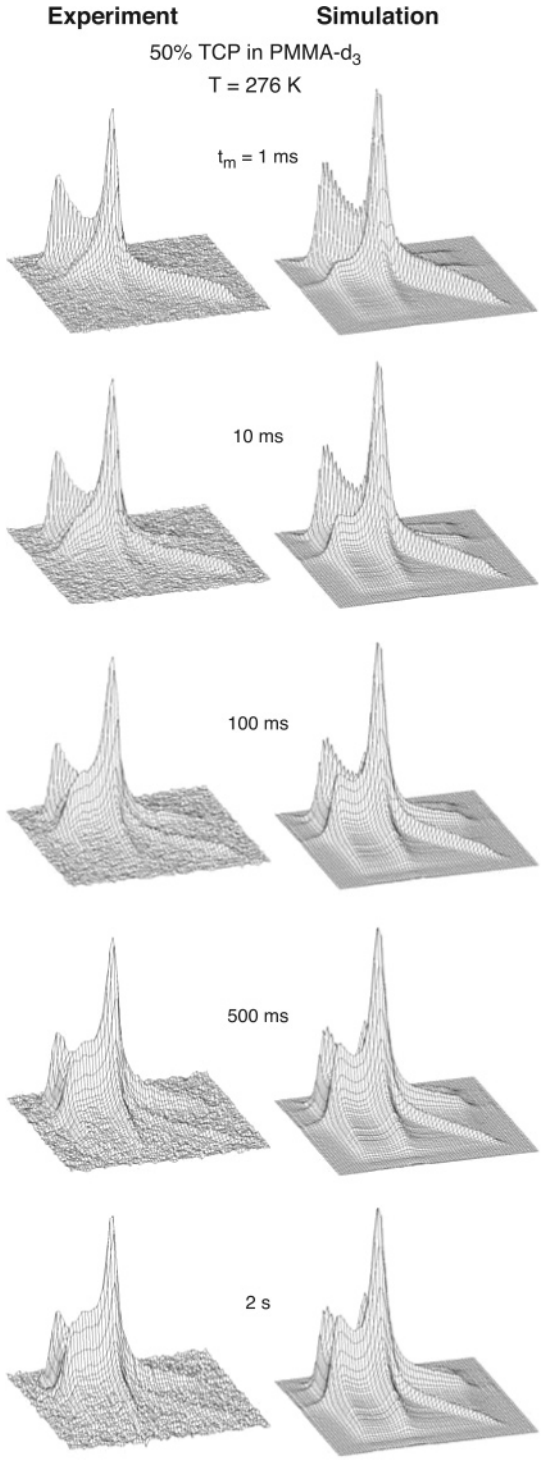

Figure 7. 2D ^{31}P NMR spectra of a 50% (w/w) mixture of tri-*m*-cresyl phosphate, TCP, with PMMA-d_3 at 276 K for mixing times, t_m, ranging from 1 ms to 2 s (left, top to bottom). Simulations based on the 1D ^{31}P Hahn-echo spectrum using weighted combinations of fast-moving (liquid), slowly moving (reorienting), and immobile TCP molecules, as well as exchange between fast and slow domains are shown on the right (cf. eq 12). The frequency range depicted extends over 54 kHz along both axes.

evident from the figure, reorientation and exchange occur on similar time scales at this temperature, showing that the dynamic heterogeneities of the TCP molecules in the matrix of immobile PMMA are transient in nature.

4.4. Orientational Correlation Function for the Plasticizer Component (TCP). More quantitative information about the reorientation dynamics can be gained from stimulated echo

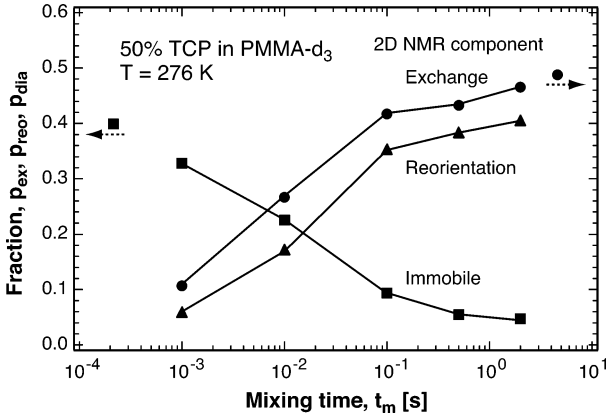

Figure 8. Weighting factors (eq 12), p_i, of the individual components in the 2D ^{31}P NMR spectra of a 50% (w/w) mixture of tri-*m*-cresyl phosphate, TCP, with PMMA-d_3 at 276 K (Figure 7) as a function of mixing time, t_m. Calculated values for the fraction of immobile molecules, p_{dia}, at $t_m = 0$ and the weighting factor for the exchange component, p_{ex}, at $t_m = \infty$ are indicated with arrows.

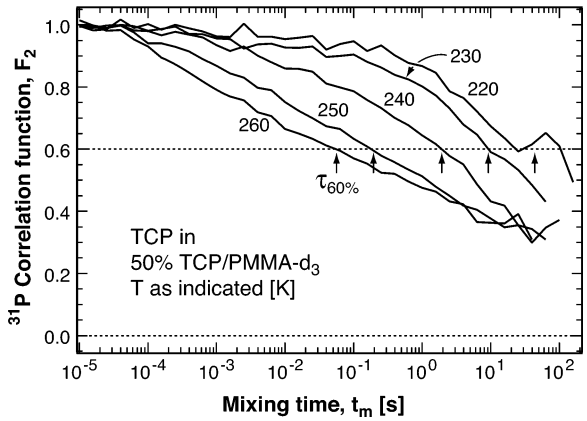

Figure 9. Orientational correlation function, $F_2(t_m)$ calculated from ^{31}P stimulated echo decays for tri-*m*-cresyl phosphate in a 50% (w/w) mixture with PMMA-d_3, from 220 to 260 K, as indicated, as a function of mixing time, t_m. Temperature-dependent correlation times, as estimated from the drop of the correlation function to 60%, are marked with arrows.

decays. We measured the sine correlation function, $F_{t_p}^{sin}(t_m)$, for the component TCP in the binary system at temperatures between 220 and 260 K with a delay time of $t_p = 15$ μs. The upper temperature is just below the onset of the liquid line in the 1D spectra (Figure 4) and comparable to the temperature of the 2D spectrum shown in Figure 6. The normalized correlation function, $\phi_{t_p}(t_m)$, (eq 4) is taken as an approximation for the orientational correlation function, $F_2(t_m)$, as shown in Figure 9. Again, because of the long T_1 time of ^{31}P, we are able to measure the correlation function for mixing times, t_m, up to about 100 s; i.e., almost 8 orders of magnitude in time is covered by the ^{31}P stimulated echo method. Even after tens of seconds the orientational correlation only decays to about half of its initial value in the temperature range investigated.

At the longest times, spin-diffusion could lead to an exchange of magnetization without motion[38] and could possibly contribute to the loss of echo signal, especially at the lowest temperatures (with the slowest relaxation). This effect does not just accelerate the signal decay, it also changes the shape of the experimental echo signal to a more exponential decay, as observed in Figure 9. We therefore limit the discussion of the shape of the correlation function to the two highest temperatures investigated, where the decay occurs in a time interval for which possible signal loss due to spin diffusion can essentially be ignored.

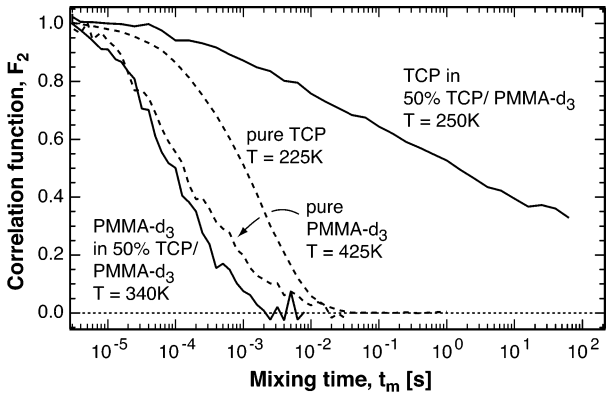

Figure 10. Comparison of the orientational correlation function, $F_2(t_m)$, as a function of mixing time, t_m, for pure PMMA-d_3, (left, dashed), PMMA-d_3 in a 50% (w/w) mixture with tri-*m*-cresyl phosphate, TCP, (left, solid), pure TCP (right, dashed), and TCP in a 50% (w/w) mixture with PMMA-d_3 (right, solid).

The most striking feature of the correlation functions for TCP in the binary system is the extreme stretching in stark contrast to the correlation function for pure TCP (Figure 10). Whereas the correlation function for pure TCP is described well with a stretched exponential function (Kohlrausch decay) with a stretching factor, β_K, of about 0.6, the correlation function of TCP in the binary mixture shows a quasi-logarithmic decay over about 3 orders of magnitude in time.

It is problematic to define a characteristic time constant for a quasi-logarithmic decay. As a simple estimate for the correlation time of TCP in the binary mixture, we determine the time at which the correlation loss has reached 0.6, as indicated in Figure 9. These time constants are compared to those for pure TCP and the polymer component in Figure 11.

4.5. Correlation Function of the Polymer Component (PMMA). Sine correlation functions for the matrix polymer PMMA in the binary mixture as well as for the pure polymer, both measured with a delay time of $t_p = 15$ μs, are shown in Figure 12. Again, we use the normalized correlation function, $\phi_{t_p}(t_m)$, as an estimate for the orientational correlation function $F_2(t_m)$ of the polymer segment. The decay functions were corrected for the quadrupolar relaxation time, T_{1Q}, and for the final correlation value, $F_\infty(t_p)$ (eqs 3 and 4). Since T_{1Q} is only about 10 ms for PMMA in the temperature range of our experiments, the accessible mixing time range is very limited. Nevertheless, the upper portion of Figure 12 shows that no matrix dynamics are observable up to 10 ms in the mixture at temperatures (290 K) for which some of the embedded component TCP already exhibits fast orientational motion on a microsecond time scale.

The correlation functions for PMMA in the binary system can be approximated by a stretched exponential function with a common stretching parameter, β_K, of 0.33. This value is comparable to the stretching parameter for the correlation functions of pure PMMA for which we find $\beta_K = 0.36$ at temperatures that are about 90−100 K higher. The similarity of the correlation decays for PMMA in the mixture and as a pure component is also evident in their direct comparison (Figure 10). Thus, it appears that the dynamics of the polymer component is simply accelerated while the shape of the correlation function is not altered significantly by the plasticizer, in pronounced contrast to the changes in the dynamics of the plasticizer itself upon embedding in the polymer matrix. This result was already anticipated in previous work.[8,17,18]

The correlation times of TCP and PMMA as pure substances and as components of the binary mixture are compared in

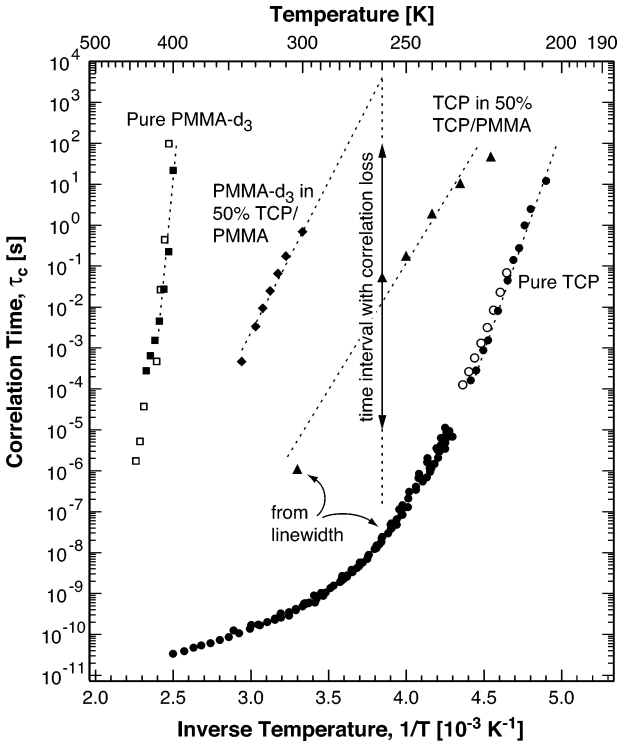

Figure 11. Comparison of the correlation times for pure PMMA-d_3 (squares), PMMA-d_3 in a 50% (w/w) mixture with tri-*m*-cresyl phosphate, TCP (diamonds), TCP in a 50% (w/w) mixture with PMMA (triangles), and pure TCP (circles) obtained from stimulated echo and relaxation experiments as a function of temperature. The time interval over which TCP relaxation was observed is indicated with a double-headed arrow. Also shown for comparison are the correlation times for the pure compounds obtained from dielectric experiments[39,40] (open symbols).

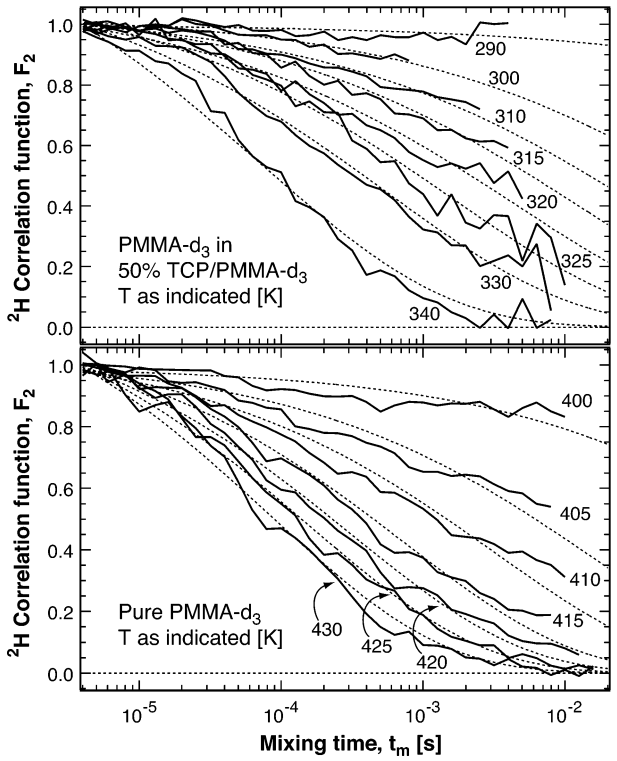

Figure 12. Top: reorientational correlation function, $F_2(t_m)$, for PMMA-d_3, in a 50% (w/w) mixture with tri-*m*-cresyl phosphate, TCP, from 290 to 340 K, as indicated, as a function of mixing time, t_m. Bottom: reorientational correlation function, $F_2(t_m)$, for pure PMMA-d_3, from 395 to 430 K, as indicated, as a function of mixing time, t_m.

Figure 11 as a function of temperature. We also added an estimate of the time constant of TCP in the mixture calculated from the width of the Lorentzian line at 303 K via $1/T_2 = 4\tau K^{CSA}/6$, with $K^{CSA} = 6/5\pi^2\delta_{CSA}{}^2$.[38] For the pure components we also included the time constants from dielectric experiments,[39,40] showing a fair agreement with our data. A strong plasticizer effect is observed for PMMA in the mixture: the correlation times shift by 90 K to lower temperatures, and their temperature dependence decreases slightly. In contrast, the time constants for TCP in the mixture are shifted to higher temperatures with respect to the correlation times of the pure compound. Again, the temperature dependence decreases in the mixture.

5. Discussion

The main results of this paper are summarized in Figures 4 and 10 for the spectra and dynamics, respectively. Our most important observation is the large qualitative difference in the dynamics of the plasticizer (TCP) in the binary system compared to its dynamics as a pure compound. While the polymer dynamics is simply shifted in temperature (or correlation time) due to plastization without discernible changes to the shape of the relaxation curve (Figure 12), the plasticizer relaxation itself changes from a stretched exponential decay to an extremely stretched-out relaxation curve (Figure 10), which cannot be fitted with a stretched exponential decay anymore. Over several orders of magnitude in time the correlation loss exhibits a quasi-logarithmic decay.

This behavior is strikingly similar to the simulation results by Moreno and Colmenero[25,26] for a binary mixture with very different mobilities for the two components. As in their simulations, we do not observe any significant motion of the polymer matrix at temperatures for which the fast component (TCP) displays logarithmic decay, as shown in Figures 4 and 12 for large-angle motion and Figure 5 for small-angle fluctuations. The dynamics of the two components appears to be completely decoupled, and separate glass transition temperatures could be assigned to each component.[24,41]

Because of the extreme stretching of the correlation function of TCP molecules in the mixture, we observe correlation loss in the entire experimentally accessible time window extending up to about 100 s. Characterizing this relaxation with a single correlation time as in Figure 11 might therefore be deceptive, as for one a logarithmic decay lacks a true correlation time and second the correlation decay displayed in Figure 9 is not yet complete at 100 s. Given the broad distribution of correlation times $G(\ln \tau)$ for TCP in PMMA, we therefore also indicate in Figure 11 the entire time interval over which correlation loss was observed in the stimulated echo decays for TCP.

Using a simple linear extrapolation of the time constant for PMMA in the mixture to lower temperatures, we estimate a correlation time of $\sim 10^4$ s for PMMA at about 260 K, the highest temperature for which the correlation function for TCP was determined. It is conceivable that this estimated correlation time for PMMA might constitute an upper bound for the very broad distribution of correlation times for TCP molecules. Such a scenario is also compatible with the correlation functions of the components reported in the simulations.[25,26] The lower experimentally accessible limit of the correlation times is given by the shortest possible waiting time of the stimulated echo technique, about 10^{-5} s. The emerging liquid line in the 1D spectrum of TCP in the binary mixture at 273 K (Figure 4) is evidence for the presence of a significant fraction of TCP

molecules with correlation times shorter than 10^{-7} s at this slightly higher temperature.

Consequently, it may be misleading to distinguish between two separate glass transition phenomena or two distinct glass transition temperatures for the binary mixture as done in Figure 11 by assigning separate time constants to the individual components. Rather, the dynamics of the mobile component covers a very broad time range, extending from close to the correlation time for the neat component potentially up to the time scale of the polymer dynamics, the latter being accelerated by the plasticizer effect. This interpretation is qualitatively consistent with the very broad "glass step" observed in the DSC traces. However, in the quantitative comparison some discrepancies appear that are not yet understood. For example, extrapolating the correlation times of PMMA in the mixture to a time constant of 100 s, we expect a glass transition temperature of about 275 K, which is well below the high-temperature end of the "glass step" in the DSC curves (Figure 3) at $T_G = 297$ K. On the other hand, the fast tail of the relaxation time distribution in the binary system, as characterized by the TCP time constant displayed in Figure 11, seems to reach 100 s at about 226 K, which is above the onset of the DSC "glass step" at $T_g = 212$ K. In other words, T_g defines as expected the temperature at which all TCP molecules in the mixture reorient with a time constant slower than 100 s.

In accordance with the simulations,[25,26] our results also show standard relaxation behavior for the polymer component in the mixture. The shape of the PMMA correlation function in the binary mixture is practically unchanged from the pure polymer dynamics and is described well with a Kohlrausch decay. Adding the TCP plasticizer simply shifts the relaxation curve to an ∼90 K lower temperature, which is consistent with DSC, dielectric, and neutron scattering experiments.[9,10,42] As the plasticizer behaves like a liquid at the temperatures for which we observe relaxation in PMMA, one might consider it a lubricant for the polymer dynamics, separating chain segments, thus easing their motion past each other.

On the basis of concentration fluctuation models[19,20] for binary systems, one might expect that the distribution of correlation times, $G(\ln \tau)$, for PMMA would broaden upon plastication, which in turn would lead to a smaller stretching parameter, β_K. However, unaltered (or even narrowed) peak shapes were observed for example in the binary system polybutadiene/mineral oil[43] and in molecular dynamics simulations of a polymer blend.[44] These virtually unchanged dynamics (compared to the pure components) have been shown to be consistent[45] with a theoretical model[46] for polymer blends.

Our 2D exchange spectra reveal that the dynamic heterogeneities of the plasticizer molecules are transient in nature. TCP molecules exchange their correlation times on a time scale similar to that of the isotropic reorientation itself (Figure 8), and no long-lived heterogeneities are observed. This observation is consistent with experiments on neat[17,47−49] and binary glass-formers, even for low molecular weight matrices.[8,14,17,18] Long-lived heterogeneities were observed very close to the glass transition temperature[50,51] for relaxation times that are too long for the NMR techniques used in this study, and there is still some controversy about whether they exist at all.[48] As we do not observe any large-scale motion of the polymer matrix below 290 K (Figure 12) but only small-angle motion (Figure 5), we conclude that these transient heterogeneities of the plasticizer molecule occur in a rigid polymer matrix.

The confinement of the plasticizer molecules in the polymer matrix may be compared to the dynamics of small molecules in other nanoconfinements, for example in zeoliths or MCM porous material.[15,52,53] While the mobile molecules experience a considerable broadening of their response function in any of these confinements, as shown for example by similar "two-phase" NMR spectra, exchange between fast and slow domains is only observed for guest molecules in a polymer matrix, even if the matrix is rigid as in the current study.

We proposed previously[16] that isotropic reorientation of plasticizer molecules is a consequence of their translational diffusion through the polymer matrix. However, it appears difficult to picture a molecular mechanism that enables the diffusion of a molecule as large as TCP in a polymer whose segments are much smaller than the diffusing molecule. On the other hand, translational "jump" diffusion of plasticizer molecules through polymers has been studied in a number of systems[54−63] and is of significant technical concern.

Analyzing the dependence of stimulated echo decays on the delay time, t_p, reveals further details about the mechanism of the molecular reorientation.[17,18] In such a study[16] we found that the isotropic reorientation of benzene in the matrix oligostyrene occurs in random jumps, as no dependence on the delay time, t_p, was observed, which may be consistent with translational diffusion causing the reorientation. However, preliminary ^{31}P NMR results on TCP in PMMA show a very strong dependence of the stimulated echo decay on the delay time, t_p, which contradicts a random jump mechanism.

6. Conclusions

Our NMR investigation of PMMA plasticized with TCP confirms predictions from recent calculations simulating binary glass-formers with kinetically constrained models.[25,26] First, the correlation function for the plasticizer TCP in the binary system is, compared to pure TCP, highly stretched out, indicating a broadening of the distribution of relaxation times due to the polymer matrix. The wings of this distribution seem to reach almost from the time scale of the dynamics of the pure plasticizer to the relaxation times of the plasticized polymer.

Second, the plasticizer TCP reorients isotropically even in a rigid PMMA matrix well below the calorimetric softening temperature of the matrix itself.

Third, while the qualitative features of the dynamics of the fast component are changed dramatically due to the presence of the matrix, the dynamics of the slow component (the polymer matrix itself) are practically unchanged, except for a large shift in temperature compared to the pure polymer. The plasticizer only seems to act as a solventlike lubricant for the polymer, lowering the glass transition temperature, while leaving the qualitative features of its segmental dynamics unchanged.

Finally, we find short-lived dynamic heterogeneities for the fast component in the binary mixture, which exchange at a rate comparable to the orientational relaxation itself.

Only the very large time window of 2D ^{31}P NMR, which is several orders of magnitude broader than that of ^{2}H NMR, made it possible to observe the highly broadened dynamics of the TCP additive in a matrix of PMMA.

Acknowledgment. Support from the German research foundation (DFG) through the Sonderforschungsbereich SFB 481 is gratefully acknowledged.

References and Notes

(1) *Kirk-Othmer Encyclopedia of Chemical Technology*, 5th ed.; Wiley-Interscience: Hoboken, NJ, 2004.
(2) Häckel, M.; Kador, L.; Kropp, D.; Frenz, C.; Schmidt, H. W. *Adv. Funct. Mater.* **2005**, *15*, 1722.

(3) Alegria, A.; Elizetxea, C.; Cendoya, I.; Colmenero, J. *Macromolecules* **1995**, *28*, 8819.
(4) Kanetakis, J.; Fytas, G.; Kremer, F.; Pakula, T. *Macromolecules* **1992**, *25*, 3484.
(5) Hirose, Y.; Urakawa, O.; Adachi, K. *Macromolecules* **2003**, *36*, 3699.
(6) Nakazawa, M.; Urakawa, O.; Adachi, K. *Macromolecules* **2000**, *33*, 7898.
(7) Alegria, A.; Colmenero, J.; Ngai, K. L.; Roland, C. M. *Macromolecules* **1994**, *27*, 4486.
(8) Blochowicz, T.; Karle, C.; Kudlik, A.; Medick, P.; Roggatz, I.; Vogel, M.; Tschirwitz, C.; Wolber, J.; Senker, J.; Rössler, E. A. *J. Phys. Chem. B* **1999**, *103*, 4032.
(9) Ceccorulli, G.; Pizzoli, M.; Scandola, M. *Polymer* **1987**, *28*, 2077.
(10) Scandola, M.; Ceccorulli, G.; Pizzoli, M. *Polymer* **1987**, *28*, 2081.
(11) Pizzoli, M.; Scandola, M.; Ceccorulli, G. *Eur. Polym. J.* **1987**, *23*, 843.
(12) Taniguchi, N.; Urakawa, O.; Adachi, K. *Macromolecules* **2004**, *37*, 7832.
(13) Savin, D. A.; Larson, A. M.; Lodge, T. P. *J. Polym. Sci., Part B: Polym. Phys.* **2004**, *42*, 1155.
(14) Vogel, M.; Rössler, E. A. *J. Phys. Chem. A* **1998**, *102*, 2102.
(15) Medick, P.; Blochowicz, T.; Vogel, M.; Rössler, E. A. *J. Non-Cryst. Solids* **2002**, *307*, 565.
(16) Medick, P.; Vogel, M.; Rössler, E. A. *J. Magn. Reson.* **2002**, *159*, 126.
(17) Böhmer, R.; Diezemann, G.; Hinze, G.; Rössler, E. A. *Prog. Nucl. Magn. Reson. Spectrosc.* **2001**, *39*, 191.
(18) Vogel, M.; Medick, P.; Rössler, E. A. *Annual Report on NMR Spectroscopy*; Academic Press: New York, 2005; p 231.
(19) Zetsche, A.; Fischer, E. W. *Acta Polym.* **1994**, *45*, 168.
(20) Roland, C. M.; Ngai, K. L. *Macromolecules* **1991**, *24*, 2261.
(21) Ngai, K. L.; Roland, C. M. *Macromolecules* **1995**, *28*, 4033.
(22) Chung, G. C.; Kornfield, J. A.; Smith, S. D. *Macromolecules* **1994**, *27*, 5729.
(23) Lodge, T. P.; McLeish, T. C. B. *Macromolecules* **2000**, *33*, 5278.
(24) Chung, G. C.; Kornfield, J. A.; Smith, S. D. *Macromolecules* **1994**, *27*, 964.
(25) Moreno, A. J.; Colmenero, J. *J. Chem. Phys.* **2006**, *125*, 016101.
(26) Moreno, A. J.; Colmenero, J. *J. Chem. Phys.* **2006**, *124*, 184906.
(27) Bergquist, P.; Zhu, Y.; Jones, A. A.; Inglefield, P. T. *Macromolecules* **1999**, *32*, 7925.
(28) Geissler, P. L.; Reichman, D. R. *Phys. Rev. E* **2005**, *71*, 031206.
(29) Genix, A. C.; Arbe, A.; Alvarez, F.; Colmenero, J.; Willner, L.; Richter, D. *Phys. Rev. E* **2005**, *72*, 031808.
(30) Sperl, M. *Phys. Rev. E* **2003**, *68*, 031405.
(31) Rössler, E. A.; Eiermann, P. *J. Chem. Phys.* **1994**, *100*, 5237.
(32) Pake, G. E. *J. Chem. Phys.* **1948**, *16*, 327.
(33) Fujara, F.; Wefing, S.; Spiess, H. W. *J. Chem. Phys.* **1986**, *84*, 4579.
(34) Schmidt-Rohr, K.; Spiess, H. W. *Multidimensional Solid-State NMR and Polymers*; Academic Press: New York, 1994.
(35) Schaefer, D.; Leisen, J.; Spiess, H. W. *J. Magn. Reson., Ser. A* **1995**, *115*, 60.
(36) Vogel, M.; Rössler, E. A. *J. Chem. Phys.* **2001**, *114*, 5802.
(37) Vogel, M.; Rössler, E. A. *J. Phys. Chem. B* **2000**, *104*, 4285.
(38) Abragam, A. *The Principles of Nuclear Magnetism;* Clarendon Press: Oxford, 1961.
(39) Bergman, R.; Alvarez, F.; Alegria, A.; Colmenero, J. *J. Chem. Phys.* **1998**, *109*, 7546.
(40) Benkhof, S.; Kudlik, A.; Rössler, E. A., unpublished results.
(41) Miller, J. B.; McGrath, K. J.; Roland, C. M.; Trask, C. A.; Garroway, A. N. *Macromolecules* **1990**, *23*, 4543.
(42) Zorn, R.; Monkenbusch, M.; Richter, D.; Alegria, A.; Colmenero, J.; Farago, B. *J. Chem. Phys.* **2006**, *125*, 154904.
(43) Casalini, R.; Ngai, K. L.; Robertson, C. G.; Roland, C. M. *J. Polym. Sci., Part B: Polym. Phys.* **2000**, *38*, 1841.
(44) Bedrov, D.; Smith, G. D. *Macromolecules* **2005**, *38*, 10314.
(45) Ngai, K. L.; Capaccioli, S.; Roland, C. M. *Macromolecules* **2006**, *39*, 8543.
(46) Ngai, K. L.; Roland, C. M. *Rubber Chem. Technol.* **2004**, *77*, 579.
(47) Kuebler, S. C.; Heuer, A.; Spiess, H. W. *Phys. Rev. E* **1997**, *56*, 741.
(48) Qi, F.; El Goresy, T.; Böhmer, R.; Doss, A.; Diezemann, G.; Hinze, G.; Sillescu, H.; Blochowicz, T.; Gainaru, C.; Rössler, E. A.; Zimmermann, H. *J. Chem. Phys.* **2003**, *118*, 7431.
(49) Böhmer, R.; Chamberlin, R. V.; Diezemann, G.; Geil, B.; Heuer, A.; Hinze, G.; Kuebler, S. C.; Richert, R.; Schiener, B.; Sillescu, H.; Spiess, H. W.; Tracht, U.; Wilhelm, M. *J. Non-Cryst. Solids* **1998**, *235*, 1.
(50) Wang, C. Y.; Ediger, M. D. *J. Chem. Phys.* **2000**, *112*, 6933.
(51) Richert, R. *J. Chem. Phys.* **2001**, *115*, 1429.
(52) Lusceac, S. A.; Koplin, C.; Medick, P.; Vogel, M.; Brodie-Linder, N.; LeQuellec, C.; Alba-Simionesco, C.; Rössler, E. A. *J. Phys. Chem. B* **2004**, *108*, 16601.
(53) Masierak, W.; Emmler, T.; Gedat, E.; Schreiber, A.; Findenegg, G. H.; Buntkowsky, G. *J. Phys. Chem. B* **2004**, *108*, 18890.
(54) Bucknall, D. G.; Higgins, J. S.; Butler, S. A. *J. Polym. Sci., Part B: Polym. Phys.* **2004**, *42*, 3267.
(55) Tonge, M. P.; Stubbs, J. M.; Sundberg, D. C.; Gilbert, R. G. *Polymer* **2000**, *41*, 3659.
(56) Hall, D. B.; Hamilton, K. E.; Miller, R. D.; Torkelson, J. M. *Macromolecules* **1999**, *32*, 8052.
(57) Hall, D. B.; Torkelson, J. M. *Macromolecules* **1998**, *31*, 8817.
(58) Hall, D. B.; Deppe, D. D.; Hamilton, K. E.; Dhinojwala, A.; Torkelson, J. M. *J. Non-Cryst. Solids* **1998**, *235*, 48.
(59) Wang, C. Y.; Ediger, M. D. *Macromolecules* **1997**, *30*, 4770.
(60) Deppe, D. D.; Miller, R. D.; Torkelson, J. M. *J. Polym. Sci., Part B: Polym. Phys.* **1996**, *34*, 2987.
(61) Heuberger, G.; Sillescu, H. *J. Phys. Chem.* **1996**, *100*, 15255.
(62) Deppe, D. D.; Dhinojwala, A.; Torkelson, J. M. *Macromolecules* **1996**, *29*, 3898.
(63) Ehlich, D.; Sillescu, H. *Macromolecules* **1990**, *23*, 1600.

MA070519G